Conference on Modelling Fluid Flow (CMFF'25)
The 19th International Conference on Fluid Flow Technologies
Budapest, Hungary, August 26 - August 29, 2025

DESIGN AND DEVELOPMENT OF AN AUTOMATIC PUMP TEST RIG FOR CONDITION MONITORING OF MECHANICAL SEALS

David Heel[1], Peter Meusburger[2], Helmut Benigni[3], Johannes Bauer[4], Ferdinand Werdecker[5], Maximilian Raith[6]

[1] Corresponding author, Institute for Hydraulic Fluid Machinery, Graz University of Technology. Kopernikusgasse 24/4, A-8010 Graz, Phone: +43 (0) 316 873 7578, E-mail: david.heel@tugraz.at
[2] Institute of Hydraulic Fluidmachinery, Graz University of Technology. E-mail: peter.meusburger@tugraz.at
[3] Institute of Hydraulic Fluidmachinery, Graz University of Technology. E-mail: helmut.benigni@tugraz.at
[4] EagleBurgmann Germany, Äussere Sauerlacher Str. 6-10 D-82515 Wolfratshausen, E-mail: johannes.bauer@eagleburgmann.com
[5] EagleBurgmann Germany, Äussere Sauerlacher Str. 6-10 D-82515 Wolfratshausen, E-mail: ferdinand.werdecker@eagleburgmann.com
[6] EagleBurgmann Germany, Äussere Sauerlacher Str. 6-10 D-82515 Wolfratshausen, E-mail: maximilian.raith@eagleburgmann.com

ABSTRACT

This paper presents the design and implementation of an experimental pump test rig for investigating mechanical seals. The primary objective of the rig is to conduct long-term tests under varying operating parameters, providing a platform for developing condition monitoring systems for mechanical seals under realistic conditions. The adjustable parameters include pump speed, flow rate, system pressure, and water temperature at the pump inlet. Additionally, the design enables controlled air injection on the suction side, the simulation of dry running of the seal, and the resulting thermal shocks during automatic refilling of the circuit, allowing replication of entire industrial processes. By incorporating vibrations, shocks, and other disturbances generated by the pump, the test rig provides a more comprehensive testing environment compared to conventional spindle-based rigs. It supports both automatic and semi-automatic operation modes, enabling comprehensive evaluation of condition monitoring systems and their practical applicability.

Keywords: Automatic operation, Condition monitoring, Long-term testing, Mechanical seals, Pump test rig

NOMENCLATURE

F_N	[N]	normal force
H	[m]	head
K	[-]	wear coefficient
Q	[m^3/h]	flow rate
Re	[-]	Reynolds number
T	[$°C$]	temperature
V_{wear}	[m³]	wear volume
n	[rpm]	rational speed
p_{abs}	[Pa]	absolute pressure
p_{diff}	[Pa]	differential pressure
p_{rel}	[Pa]	relative pressure
x	[m]	distance
η	[$\%$]	efficiency
σ_0	[N/m^2]	hardness

Subscripts and Superscripts

AE	acoustic emission signal
PS, SS	pressure side, suction side

1. INTRODUCTION

Mechanical seals are high-precision sealing systems specifically developed for pressurized shaft passages. They are characterized by a very narrow sealing interface and low friction. Due to their low-maintenance design and long service life, they are widely used in pumps, compressors, propeller shafts, mixers, and filtration systems. [1,2] A study by the Fraunhofer Institute identified that the mechanical seal is one of the main reasons for the failure of pumps in industrial processes, followed by bearing and gap wear. [3]

Although mechanical seals are designed for long service lives, analysing premature failure or excessive wear remains a significant challenge. The unpredictability of such failures poses the risk of unplanned plant shutdowns, which can result in costs of several million euros per day, depending on the plant's size and production volume. [4] In many cases, repair and associated costs can surpass the initial cost of the seal by factors ranging from 100 to 1000 times. [5] Continuous condition monitoring is therefore a key research focus to detect wear and seal failure at an early stage, enabling planned maintenance and replacement cycles, and ensuring

the operational reliability and cost-effectiveness of the entire system.

Furthermore, API 682 [6], which defines the requirements for shaft sealing systems in centrifugal and rotary pumps in the field of oil-, gas- and process engineering, mandates three years of uninterrupted operation while complying with environmental emission regulations. To meet these standard requirements, condition monitoring of the mechanical seal may be essential.

The sealing interface of a mechanical seal is oriented normally to the shaft and is formed by two opposing faces. These contact surfaces are designed to allow a thin lubricating film to be established under specific operating conditions. The thickness of which significantly influences both leakage and frictional behaviour. [7] Leakage occurs radially through the sealing interface. To better understand the function of a mechanical seal, refer to Figure 1, which illustrates its schematic structure. The axially movable rotating seal face is pressed against a stationary seat by one or multiple springs. This spring ensures automatic adjustment of the sealing interface, compensating for wear and thermal expansion, thereby maintaining continuous contact between the sealing face and the seat. Material pairings such as carbon graphite combined with metal or ceramic are often selected, while O-rings are employed as secondary sealing elements. [8]

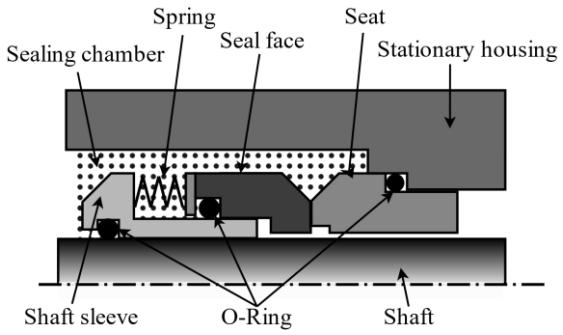

Figure 1. Schematic design of a mechanical seal

Previous efforts to develop condition monitoring systems have predominantly utilized spindle test rigs, where the seal is installed in a dedicated test setup and the shaft is driven externally. The test rig presented in this publication enables the development of condition monitoring systems directly within a pump. In addition to facilitating the design of new monitoring approaches, it also allows for the evaluation of existing condition monitoring systems. By precisely controlling the operating conditions, specific processes and events can be conducted in a reproducible manner.

2. FAILURE OF MECHANICAL SEALS

2.1. Theory of wear

When defining the tribological system of a mechanical seal based on DIN 50320 [9], the stationary seat serves as the base body, while the rotating seal face acts as the counterbody, which is subjected to the applied load. The intermediate substance is the process medium, which forms the sealing gap. Depending on the seal configuration, the process medium and, in some cases, the barrier fluid function as the environmental medium. In general, frictional states can be classified into solid-state friction, boundary friction, mixed friction, fluid friction, which includes hydrostatic, hydrodynamic, and elastohydrodynamic lubrication, as well as gas friction, which can occur under aerostatic or aerodynamic conditions.

All of these frictional states can occur within a mechanical seal, leading to different wear mechanisms. The most common wear mechanisms include adhesion, abrasion, surface fatigue, and tribochemical reactions. [7]

According to Popov [10], the dominant wear mechanism in sliding contacts is adhesive wear. Continuous stress on the sliding surfaces due to adhesive contact leads to crack formation at the welded surface unevenness. If adhesion forces become too high, particles or material grains may detach. These particles are further ground down within the sealing gap until they are flushed out, causing additional cracks and leading to material removal. [10,11] The wear volume V_{wear} can be determined using the Holm-Archard equation [12], which states that the worn volume is proportional to the normal force F_{N} and sliding distance x, while inversely proportional to the hardness σ_0 of the softer sliding partner. Manufacturers typically provide the wear coefficient K based on the material pairing.

$$V_{\text{wear}} = K \frac{F_{\text{N}} \cdot x}{\sigma_0} \tag{1}$$

2.2 Premature failure

A mechanical seal is a wear component designed for a specific service life. The primary factor used to determine its lifespan is the adhesive wear of the sealing surfaces. However, a significant amount of mechanical seals does not reach their expected service life. In such cases, the term "premature failure" is used. [13]

There are numerous reasons why a mechanical seal may fail before reaching its intended lifespan. Some of these factors occur even before the seal is put into operation, including design flaws, manufacturing defects, or installation errors. Regardless of these pre-operational issues, this discussion focuses on failure mechanisms that arise during operation. In many cases, premature failure is

caused by a combination of multiple factors rather than a single issue. [14]

2.2.1 Mechanical overload

Even with proper design and installation, a mechanical seal may experience excessive mechanical stress. One of the primary causes is operational misuse of the equipment. Excessive pressure or sliding speeds can lead to grooving on the sealing surfaces. [5] Sudden pressure surges, often resulting from the rapid closing of a valve or shut-off device, can impose shock loads on the seal, potentially causing cracks or edge chipping. Additionally, mechanical overload can be induced by pump vibrations, whereas damaged bearings may cause these vibrations. Furthermore, improper flow conditions, such as blockages, deposits, or unfavourable operating points, can lead to increased radial forces acting on the seal, further accelerating wear and failure. [15]

2.2.1 Thermal overload

One of the leading causes of thermal overload is dry running of the seal, which can lead to fluid evaporation within the seal chamber. [13] A sudden temperature change, such as flushing the system with a cold medium after a high-temperature process, can cause thermal shock. Similarly, irregular operating conditions, including frequent start-stop cycles or insufficient flushing, can result in excessive heat build-up. [16] The consequences of thermal overload include crack formation, material embrittlement, and deformation of sealing components. [17] Moreover, excessively high temperatures can also cause degradation of secondary seals such as O-Rings, leading to leakage and failure of the entire sealing system.

2.2.3 Chemical degradation

Mechanical seals are also vulnerable to chemical attacks, particularly corrosion of metallic or ceramic components. [5] Additionally, carbonization or crystallization of process media can lead to increased leakage or even complete seal failure. [8] Secondary seals, may also be compromised if the material compatibility with the process fluid is insufficient. Chemical degradation is particularly critical in aggressive operating environments where exposure to acids, solvents, or high-temperature fluids accelerates material deterioration.

3. CONDITION MONITORING FOR MECHANICAL SEALS

The condition monitoring of mechanical seals can take various forms and must be tailored to the specific application. As previously discussed, there are numerous causes of seal failure. The first step in developing an effective monitoring system is to determine which failure mechanisms should be observed. Furthermore, the focus during development should always be on application in real use cases.

A basic method for assessing the condition of a mechanical seal is leakage detection. Additional measurable parameters that provide insights into the frictional state include temperature measurements at the seal face, seat, or within the sealing gap. [18] In particular, during solid-state friction and boundary lubrication, wear is significantly increased due to the conversion of kinetic energy into heat at the tribological contact interface. As a result, the temperature of the entire tribosystem and especially the interfacial temperature rises. [9] To assess the stress conditions acting on the seal, comprising a combination of pressure and sliding velocity (pressure x velocity), it is necessary to measure the operating pressure and rotational speed of the system. [13,19]

Lambert [20] already presented a system which monitors the condition of mechanical seals by measuring operating parameters in 1998. To improve reliability, the surface temperature was calculated using a finite element method.

Beyond these basic condition monitoring techniques, measuring the lubrication film thickness within the sealing gap provides valuable information on the friction state of the sliding surfaces. By defining a critical threshold for fluid film thickness, a distinction can be made between pure fluid lubrication and solid-state contact. [19] Since the fluid film is only a few micrometers thick, the sensors used must have a very high resolution. However, measuring the lubrication film thickness is particularly challenging in transient operating conditions, where temperature variations further complicate the measurement task.

Several sensor-based measurement techniques have been investigated for determining the lubrication film thickness, for example by Zou and Green [21] using an eddy current sensor. The eddy current proximity probes were attached to the end of the housing to measure the static and dynamic distance between the seat and the end face of the rotor.

Another possibility is to use the acoustic emission signal (AE), as this can contain a lot of information on the friction of the end surfaces. Based on the operating conditions, three main mechanisms can contribute to AE generation during sliding, namely viscous friction due to the shearing of lubricant layers, the interaction between surface irregularities and fluid flows, and direct contacts of the surface irregularities. In addition to understanding the formation mechanism of tribological AEs in mechanical seals, there is a difficulty in characterizing the AE signal. [13,22]

A further option is to impose active ultrasonic waves with a piezoelectric ultrasonic transducer and compare them with the signal reflected and received

by the sliding surface. [13] Dwyer-Joyce presents in [23] the theoretical principles for the interaction of ultrasound with the interfaces and the fluid film.

The above list provides a brief overview of the possibilities for condition monitoring. There are many other promising methods. For future research, there are improvements in sensor accuracy, the integration of real-time monitoring systems, and the optimization of data analysis techniques to implement.

4. TEST RIG

The primary circuit, also referred to as the main circuit, is driven by the main pump. The test mechanical seals ensure that the medium in the main circuit is sealed against the environment and the rotating shaft of the main pump.

Following the flow direction from the main pump, the medium passes through a flow control valve (C1), which regulates the volumetric flow rate, before entering the pressure vessel. The pressure vessel serves as a damping element, with an adjustable air cushion in the upper half that allows system pressure modulation. From there, the medium continues its way through a heat exchanger, which allows precise thermal conditioning, before flowing through a dedicated pipeline section designed for controlled air injection. Finally, the medium returns to the pump inlet, closing the loop.

To simulate dry-running conditions, the pump's drainage valve (C6) can be opened, enabling controlled evacuation of the working fluid. Butterfly valves (C2) and (C3) are installed on the suction and pressure sides of the main pump. When closed, they prevent complete drainage of the system, ensuring that only the section between the valves is emptied.

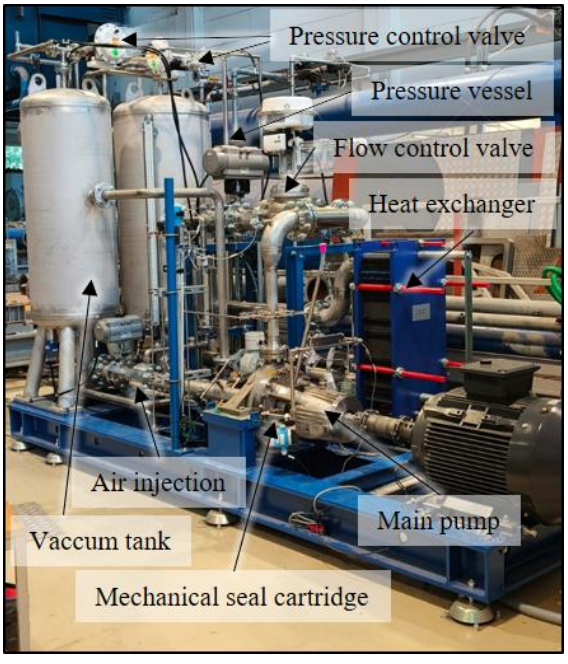

Figure 2. Test rig overview

Table 1. Control valves of the test rig

Flow control valve	C1
Butterfly valve pressure side	C2
Butterfly valve suction side	C3
Pressure boost valve	C4
Pressure relief valve	C5
Pump drain valve	C6
Air injection control valve	C7

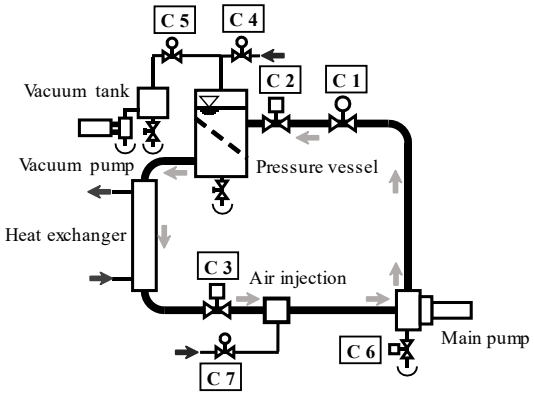

Figure 3. Schematic diagram of main test rig components

4.1 Control variables of the test rig

The test rig can operate fully automatic, with predefined process steps being executed sequentially. Alternatively, a semi-automatic mode allows for manual input of specific control variables. The following sections describe the individual control loops.

The drive motor of the main pump is controlled via a frequency converter, which regulates and monitors the motor operation. The actual speed is measured by a rotary encoder (M13) that records the rotational speed of the motor shaft.

The flow rate in the primary circuit is regulated using a proportional valve (C1). By adjusting the valve position, the volume of liquid flowing through the main circuit can be continuously controlled. A magnetic inductive flow meter (M06) is used to measure the flow rate. To ensure the possibility of reducing the flow to zero discharge, a shut-off valve is installed in the primary circuit.

The system pressure is regulated via an air cushion in the upper section of the pressure vessel. To increase pressure, compressed air from an external supply is introduced via the booster valve (C4), expanding the air cushion until the desired pressure is reached. Pressure reduction is achieved via the pressure relief valve (C5), which is connected to a vacuum tank. This allows air to be released from the pressure vessel into the vacuum tank, which is maintained at a reduced pressure by a vacuum pump. The actual system pressure is recorded by the piezoresistive pressure sensor (M03).

The temperature in the primary circuit is regulated via a heat exchanger, which dissipates excess heat. The setpoint temperature is determined by sensor (M09), a PT100 resistance thermometer. The cooling source of the system is a chiller unit, while heat is introduced into the system through the operation of the main pump.

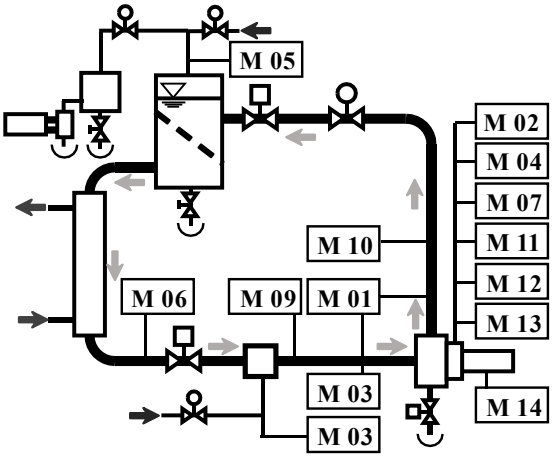

Figure 4. Diagram of the instrumentation

The test rig allows for controlled air injection into the main circuit on the suction side of the pump. This is achieved via a pipe section equipped with mixing nozzles. The pipeline assembly consists of an annular chamber with wall perforations, which is connected to a pressurized air line equipped with a check valve. The air flow rate is regulated using proportional valve (C7) and monitored via an ultrasonic flow meter (M08).

Table 2. Measured variables at the test rig

Pressure	
Differential pressure pump	M01
Relative pressure at seal	M02
Absolute pressure suction side	M03
Absolute pressure ambient	M04
Relative pressure pressure vessel	M05
Flow rate	
Main circuit	M06
Flush mechanical seal	M07
Air injection	M08
Temperatures	
Suction side	M09
Pressure side	M10
Flush mechanical seal	M11
Seal face	M12
Rotational speed	
Main pump speed	M13
Electrical power	
Main pump power	M14

4.2 Condition monitoring of the mechanical seal

As shown in Figure 4, a set of measurement variables is extracted from the main pump, representing the condition monitoring system of the mechanical seal. These measured variables include the relative pressure of the seal (M02) and the ambient pressure (M04) as key pressure parameters. The pressure connection of (M02) is shown in Figure 5. The hole ends very close to the sealing gap, the measured pressure corresponds to the pressure that the seal must also withstand. Additionally, the flow rate in the flushing line from the spiral casing to the seal is monitored using an ultrasonic flow meter (M07). Further monitoring parameters include the temperature in the flushing line (M11) and the temperature near the seal face (M12, thermocouple in Fig. 5). To complete the readings for a load collective, the rotational speed of the main pump (M13) is also recorded.

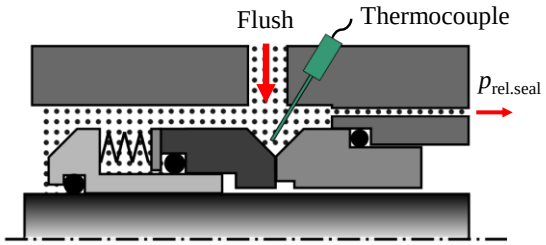

Figure 5. Instrumentation of the mechanical seal

The selected monitoring parameters represent fundamental baseline values. However, the system allows for future expansion. Before extending the monitoring setup, it is essential to determine the specific tests to be conducted on the test rig. If necessary, additional parameters can be integrated into the condition monitoring system.

5. INITIAL MEASUREMENT DATA

For this study, three measurement series were recorded, each representing a pump characteristic curve. The pump characteristics were determined at three constant rotational speeds: 1500 *rpm*, 2500 *rpm*, and 3500 *rpm* In addition, for each measurement series the system pressure was maintained at 6 *bar*, and the temperature was kept constant at 20 *°C* on the suction side of the pump.

Starting from zero discharge, the flow rate was incrementally increased in steps of 10 m^3/h until the pump's maximum achievable flow rate was reached. The pump's delivery head is determined by the before mentioned parameters.

The process sequence executed on the test rig ensures that the system is properly prepared before the actual measurement. Before recording a pump characteristic curve, the pipeline system is flushed, and the test rig is stabilized at a constant temperature

of 20 *°C*. Therefore, the main pump speed is set to 2500 *rpm*, and a flow rate of 80 *m³/h* is held constant for 200 seconds. Following this stabilization phase, an automated flushing for the pressure sensors is performed at reduced speed. After completing this step, the actual measurement process is initiated. In the final stage, the pump speed is brought to a full stop at 0 *rpm*. This standardized procedure ensures repeatable initial conditions for each test run, thereby improving the reliability and reproducibility of the measurements.

Each measurement series was recorded continuously. The measuring software sampled data at 1000 *Hz* and stored averaged values every second.

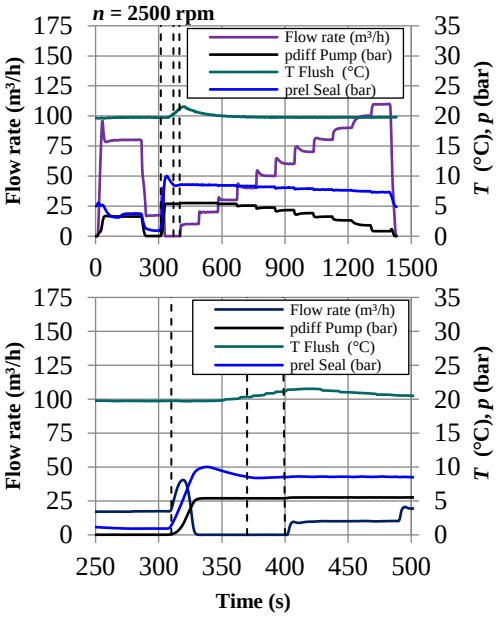

Figure 6. Continuous recording at 2500 *rpm*, (top) full measurement log (bottom) first process step

Figure 6 (top) illustrates the complete process sequence for the measurement series at 2500 *rpm*.The graph (bottom) in Figure 6 shows the time interval of the initial section of the characteristic curve at a flow rate of 0 *m³/s*. Each process step consists of a settling phase and a holding phase. This is indicated by three vertical lines: the first marks the start of the process step and the beginning of the settling phase, the second marks the transition from the settling to the holding phase, and the third marks the end of the holding phase and the completion of the process step.

During the settling phase, the control system adjusts the operating parameters until they stabilize. In the holding phase, the values reached at the end of the settling phase are maintained. If the target system pressure is 6 *bar* but only 4.5 *bar* is achieved within the predefined settling time, then 4.5 *bar* becomes the new target value for the holding phase. As a result, no significant changes occur during the holding phase, allowing for the calculation of an average value that is representative of this operating state of the pump while minimizing variance.

For the measurement series, the settling phase was set to 60 *s*, followed by a 30 *s* holding phase. In Figures 7 to 9, a mean value was calculated from the data recorded during the holding phase, representing a single measurement point.

The authors consistently present the data as a set of two graphs. The upper graph illustrates the pump characteristic curve at the respective rotational speed, along with the pump efficiency and the measured electrical power, compensated by the efficiency of the drive motor. By analysing the pump characteristic curve, its power and its efficiency, the operating point of the pump can be assessed. This evaluation also serves to associate the data related to the seal, which is depicted in the lower graph. For the seal-related data, the selected parameters include the sealed pressure, as well as the flow rate and temperature of the flushing medium. All data is plotted against the flow rate. Based on these representations, the following section analyses the trends observed in the measurement data, focusing on the interaction between pump and seal.

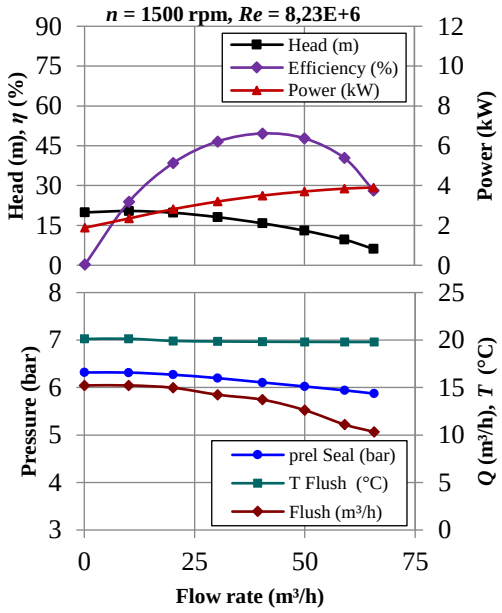

Figure 7. (top) Pump characteristic 1500 *rpm*, (bottom) corresponding measured variables

The results, as shown in Figure 7, illustrate the pump's performance at a rotational speed of 1500 *rpm*. At this speed, the pump reaches a maximum head of 20.4 *m* and a maximum flow rate of 65 *m³/h*, with a peak efficiency of 49.6 *%*. Examining the head curve from the first measurement series reveals that the second measurement point is slightly above the first. Gülich [24] describes characteristic curves where the gradient $\partial H/\partial Q > 0$ is as "unstable." The drop in head at very low flow rates can be attributed to

recirculation within the impeller, a typical behaviour for centrifugal pumps of this specific speed and design. The power and efficiency curves both follow the expected trends.

The relative pressure at the seal decreases as the flow rate increases, which is expected since the pump head also decreases. Notably, the entire pressure generated by the pump does not appear at the seal. This drop in measured static pressure can be explained by the dynamic pressure component, which is influenced by the seal flushing. The dynamic pressure reduction occurs due to the flushing flow, which follows an inverse trend compared to the main pump flow. The flushing line functions as a bypass from the spiral casing to the seal, meaning that the higher the differential pressure generated by the pump, the higher the flushing flow rate. The temperature of the flushing flow remains constant at 20 °C, which is consistent with the suction-side temperature regulation of the pump.

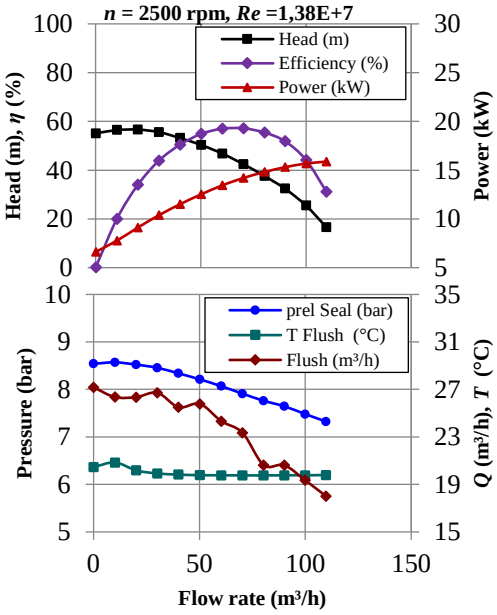

Figure 8. (top) Pump characteristic 2500 *rpm*, (bottom) corresponding measured variables

Figure 8 presents the data from the measurement series at 2500 *rpm*. At this rotational speed, the pump achieves a maximum head of 56.6 *m* and a maximum flow rate of 109.7 *m³/h*. By applying the similarity laws according to EN ISO 9906:2012 [25] or IEC 60193:2019 [26], similar operating points can be converted. In this context, the flow rate scales linearly to the speed ratio, the head scales to the square of the speed ratio, and the power scales to the cube of the speed ratio. Applying these laws to the measurement data reveals a good correlation between the first and second measurement series.

The pump reaches a peak efficiency of 57.2 %, which is significantly higher than the efficiency measured in the first series. According to IEC 60193 [26], the frictional losses in the flow of hydraulic machinery are primarily dependent on the Reynolds number (*Re*). Since the Reynolds number increases by approximately 1.7 times due to the higher rotational speed, an increase in efficiency is also expected. It should be noted: In the evaluation, the outlet diameter of the impeller was used as the characteristic length for calculating the Reynolds number displayed in Figure 7 to 10.

The unstable characteristic curve can be recognized even more clearly. The relative pressure at the seal follows a trend similar to that observed in the first measurement series, and the unstable nature of the pump characteristic curve is also evident in the pressure profile. The temperature of the flush remains at approximately 20 °C, with a slight increase observed at very low flow rates. This temperature rise occurs because, at this operating point, heat accumulates due to insufficient dissipation caused by the low flow rate. Examining the temporal progression in Figure 6 shows a continuous temperature increase once a flow rate of 0 m³/h is reached. As previously discussed, the standardized startup process ensures that this temperature increase does not originate from prior process conditions.

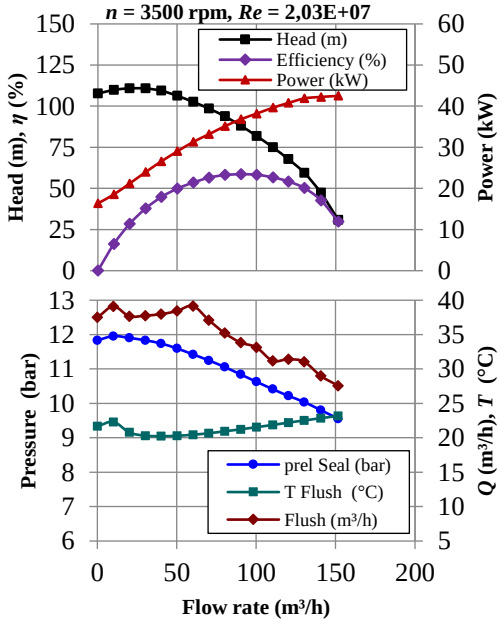

Figure 9. (top) Pump characteristic 3500 *rpm*, (bottom) corresponding measured variables

The data from the latest measurement series at 3500 *rpm* are shown in Figure 9. At this rotational speed, the pump achieves a maximum head of 110.9 *m*, a maximum flow rate of 151.6 *m³/h*, and a peak efficiency of 58.7%. The correlation based on the similarity laws aligns very well with the other measurement series. The trend of the relative pressure at the seal and the flushing flow rate fits the overall pattern. The temperature profile of the

flushing flow shows a slight increase at very low flow rates, subsequently drops back to 20 °*C*, and then rises steadily. A possible explanation for this behaviour could be the power increase, which scales with the cube of the rotational speed ratio. This causes the pump housing and the cartridge to heat up over time until a thermal equilibrium is reached.

To complement the presented measurement results, Table 3 provides quantified uncertainty values for the displayed parameters. The uncertainty analysis follows DIN EN ISO 99006 [25], using representative values near the pump's best efficiency point. Measurement uncertainty may vary across the measurement range, particularly at its boundaries, where deviations tend to be more pronounced. The primary objective is to provide a quantitative estimate of the uncertainty associated with the reported values.

The analysis accounts for the entire measurement chain, including the data acquisition system, galvanic isolation amplifiers, signal conditioners, and the respective sensors. The reported uncertainties represent expanded uncertainties with a confidence level of 95 %. The current setup meets the grade 1 acceptance criteria for pump measurements according to DIN EN ISO 9906 [25].

Table 3. Measurement uncertainty

Head	0.7118 %
Flow rate	0.8684 %
Efficiency	1.7335 %
Power	1.3207 %
Relative pressure at seal	0.7954 %
Temperature flush	0.8211 %
Flow rate flush	1.5793 %

6. SUMMARY

Monitoring the condition of mechanical seals is essential for detecting wear and failures, ensuring operational reliability, and enabling early intervention. To develop and validate existing condition monitoring approaches for mechanical seals, a dedicated test rig was designed and constructed. The test rig allows precise control over key operating parameters, including pump speed, flow rate, system pressure, and water temperature at the pump inlet. Additionally, its design enables controlled air injection on the suction side, the simulation of seal dry-running conditions, and the resulting thermal shocks upon automatic refilling of the circuit. These features allow the replication of entire industrial processes under controlled conditions. Initial measurements were recorded and analysed using the pump performance curve as a reference.

The presented test rig provides a solid foundation for further investigations, particularly long-term tests. Moreover, it can be employed to diagnose application-specific issues by replicating real-world processes in a controlled laboratory environment and applying appropriate measurement techniques to identify the root cause. The setup also facilitates the validation of existing condition monitoring systems, making it a versatile tool for research and practical applications. Future work will focus on optimizing the measurement techniques and further expanding the range of monitored parameters to further enhance the reliability of mechanical seal condition monitoring.

ACKNOWLEDGEMENTS

This work has been supported by the EagleBurgmann Germany GmbH & Co. KG.

AUTHORS' CONTRIBUTION

All authors were involved in the conception and design of this study. D.H. was responsible for material preparation, data collection, and analysis. D.H. wrote the first draft of the manuscript, and all other authors provided feedback on previous versions. All authors read and approved the final manuscript.

REFERENCES

[1] Schlegel R., 1984, "Gleitringdichtungen für Pumpen in der chemischen Industrie", Chemie Ingenieur Technik, Vol. 56(5), pp. 397–399.

[2] Zhang Z., Chen K., Zhang E. Q., and Fu P., 2014, "Mechanical Seal Condition Monitoring Technology Research", AMM, Vol. 529, pp. 344–348.

[3] Kohlmann B., and Schneider S., 2007, "Zuverlässigkeitsprognose von mechatronischen Systemen zur Ableitung restnutzungsdauerbezogener Betriebs- und Instandhaltungsstrategien".

[4] SIEMENS AG, 2024, "The True Cost of Downtime 2024", https://assets.new.siemens.com/siemens/assets/api/uuid:1b43afb5-2d07-47f7-9eb7-893fe7d0bc59/TCOD-2024_original.pdf.

[5] Riedl A., Ed., 2017. *Handbuch Dichtungspraxis*, 4th ed., Vulkan Verlag, Essen.

[6] American Petroleum Institute, 2014, "Pumps—Shaft Sealing Systems for Centrifugal and Rotary Pumps" API STANDARD 682.

[7] Czichos H., and Habig K.-H., 2020. *Tribologie-Handbuch*, Springer Fachmedien Wiesbaden, Wiesbaden.

[8] Müller H., and Nau B., 2024, "Gleitringdichtungen: Grundlagen", www.fachwissen-dichtungstechnik.de.

[9] DIN Deutsches Insitut für Normen, 1979, "DIN 50320: Verschleiß; Begriffe,

Systemanalyse von Verschleißvorgängen, Gliederung des Verschleißgebietes" Deutche Normen.
[10] Popov V. L., 2015. *Kontaktmechanik und Reibung*, Springer Berlin Heidelberg, Berlin, Heidelberg.
[11] Ni X., Sun J., Ma C., and Zhang Y., 2023, "Wear Model of a Mechanical Seal Based on Piecewise Fractal Theory", Fractal Fract, Vol. 7(3), p. 251.
[12] Archard J. F., 1953, "Contact and Rubbing of Flat Surfaces", Journal of Applied Physics, Vol. 24(8), pp. 981–988.
[13] Fan Y. E., Gu F., and Ball A., 2008, "A Review of the Condition Monitoring of Mechanical Seals", ASME 7th Biennial Conference on Engineering Systems Design and Analysis, pp. 179–184.
[14] Plumridge J., and Page R.L, The development of more tolerant mechanical seals, *Shaft sealing in centrifugal pumps*, pp. 9–22.
[15] Shiels S., 2002, "Failure of mechanical seals in centrifugal pumps — part two", World Pumps, Vol. 2002(432), pp. 34–37.
[16] Shiels S., 2002, "Failure of mechanical seals in centrifugal pumps", World Pumps, Vol. 2002(429), pp. 20–22.
[17] Mayer E., 1960, "Doppeltwirkende axiale Gleitringdichtungen in der chemischen Industrie", Chemie Ingenieur Technik, Vol. 32(4), pp. 285–288.
[18] Fan Y. E., 2007. *The condition monitoring of mechanical seals using acoustic emissions*.
[19] Gu F., Towsyfyan H., and Ball A., 2013. *A review of mechanical seal tribology and condition monitoring*, University of Huddersfield, Huddersfield.
[20] Lambert P., 1998, "A condition-based monitoring system for mechanical seals", Sealing Technology, Vol. 1998(57), pp. 7–9.
[21] Zou M., and Green I., 1998, Real-time Condition Monitoring of Mechanical Face Seal, *Tribology for energy conservation: Proceedings of the 24th Leeds-Lyon Symposium on Tribology, held in the Imperial College of Science, Technology, and Medicine, London, UK, 4th-6th September 1997*, Dowson D., ed., Elsevier for the Institute of Tribology University of Leeds and Institut National des Sciences Appliquées de Lyon, Amsterdam, New York, pp. 423–430.
[22] Towsyfyan H., Gu F., Ball A. D., and Liang B., 2019, "Tribological behaviour diagnostic and fault detection of mechanical seals based on acoustic emission measurements", Friction, Vol. 7(6), pp. 572–586.
[23] Dwyer-Joyce R. S., 2005, "The Application of Ultrasonic NDT Techniques in Tribology", Proceedings of the Institution of Mechanical Engineers, Part J: Journal of Engineering Tribology, Vol. 219(5), pp. 347–366.
[24] Gülich J. F., 2020. *Centrifugal Pumps*, Springer International Publishing, Cham.
[25] EUROPEAN COMMITTEE FOR STANDARDIZATION, "DIN EN ISO 9906:2013-03, Kreiselpumpen_- Hydraulische Abnahmeprüfungen_- Klassen_1, 2 und_3 (ISO_9906:2012); Deutsche Fassung EN_ISO_9906:2012".
[26] International Electrotechnical Commission, 2019, "IEC 60193:2019: Hydraulic turbines, storage pumps and pump-turbines – Model acceptance tests" International Standard.